Journal of Applied Electrochemistry (2006) 36:677–683
DOI 10.1007/s10800-006-9123-1

Removal of Pb(II) from simulated wastewaters using a stainless-steel wool cathode in a flow-through cell

LUIZ H.S. GASPAROTTO, NERILSO BOCCHI*, ROMEU C. ROCHA-FILHO and SONIA R. BIAGGIO
*Departamento de Química, Universidade Federal de São Carlos, Caixa Postal 676, 13560-970, São Carlos, SP, Brazil (*author for correspondence, tel.: +55-16-3351-8079, fax: +55-16-3351-8350, e-mail: bocchi@dq.ufscar.br)*

Received 22 August 2005; accepted in revised form 12 January 2006

Key words: electrolytic wastewater treatment, flow-through cell, lead, stainless-steel wool, three-dimensional cathode

Abstract

The investigation of an electrolytic process to remove Pb(II) from simulated wastewaters using a stainless-steel wool (SSW) cathode in a flow-through cell under potentiostatic condition is reported. Voltammetry under hydrodynamic conditions was used to estimate the diffusion coefficient, which was found to be 1.4×10^{-5} cm^2 s^{-1} in the supporting electrolyte (0.10 mol l^{-1} $NaNO_3$ and 0.10 mol l^{-1} H_3BO_3, pH 4.8). The performance of the flow-through cell was evaluated for three potentials: −0.70, −0.80 and −0.90 V vs. saturated calomel electrode (SCE). At −0.70 V, the reaction was found not to be completely controlled by mass transfer, while at −0.80 V and −0.90 V the Pb(II) concentration decayed exponentially. At −0.90 V, using a flow rate of 250 l h^{-1}, after a 90-min electrolysis, the Pb(II) concentration decayed from 50 ppm to only 1 ppm, corresponding to a 98% removal.

1. Introduction

Lead is a non-ferrous metal largely used in soil pipes, batteries (alloyed with antimony), paints and different alloys. Its largest use is in lead-acid batteries because of characteristics such as good conductivity, resistance to corrosion and the reversibility of the reaction between lead oxide and sulphuric acid [1]. Wastewater generated during the processing of lead-acid batteries contains Pb(II), which is very toxic to the environment and to living beings. Thus, before discharging this wastewater into sewers, effluent treatment must be carried out in order to decrease the concentration of the metallic ion.

Aqueous effluents are conventionally treated by chemical precipitation of insoluble salts and hydroxides. This method is efficient for some metals, but its major drawback is the large amount of sludge that remains after treatment; the appropriate disposal of this sludge leads to a significant cost increase for the industry. Electrochemical technology can provide an efficient way of treating wastewater as it can remove pollutants producing no by-products [2]. As an example, electrolysis can be used to recover metals from industrial effluents [3]. However, most electrolytic processes are ineffective at low ion concentrations due to the low mass transfer rate of the metal ions from the solution to the cathode surface [4].

Three-dimensional porous cathodes, as well as the materials used for this purpose, have been extensively studied throughout the years [5–11]. The percolation of the electrolyte through these cathodes allows the achievement of both large electrode surface areas and high mass transfer rates for the electrochemical reactions. Ponce de Leon and Pletcher [12] investigated the removal of Pb(II) from different aqueous electrolytes at pH 2 using reticulated vitreous carbon (RVC) as a cathode and showed that the ion removal was always possible in perchlorate, nitrate, tetrafluoroborate and chloride media. Bertazzoli et al. [13] reported that the use of RVC cathodes of 20, 45, 60 and 80 pores per inch, under a potentiostatic condition, led to a reduction of the Pb(II) concentration from 50 to 0.1 ppm, for recirculation times ranging from 20 to 120 min depending on the RVC porosity and the flow-rate.

Stainless steel has also proved to be very effective as a cathode for metal removal from wastewater [14, 15]. Paidar et al. [16] used stainless-steel wool (SSW) and graphite felt to simultaneously remove Cu(II) and Zn(II) from diluted solutions. This material showed a good stability as cathode and could also be anodically polarized during its regeneration process without damage, something RVC and graphite cannot withstand [16]. Furthermore, stainless steel is an inexpensive material when compared to graphite felt. Barbosa et al. [17] used a mild steel wool and a stainless-steel mesh coil for gold electrowinning and they found that electrolyte recirculation enhanced the gold recovery from the diluted liquors. Elsherief [18] developed a flow-by cell

with a spiral wound steel electrode for Cd(II) electrowinning. For a 250-ml solution volume and optimized operating conditions, the Cd(II) concentration was decreased from 500 ppm to less than 5 ppm in 90 min.

As far as is known, SSW has not been employed for the removal of Pb(II) from wastewaters. In this work an electrochemical process under potentiostatic conditions was carried out using a SSW cathode in a flow-through cell for the removal of Pb(II) from simulated wastewaters.

2. Experimental

2.1. *Chemicals*

All the reagents used in this work were of analytical grade and the solutions were prepared using distilled and deionized water. The solutions with different Pb(II) concentrations were prepared adding appropriate volumes of a stock solution of lead nitrate [5 g l^{-1} Pb(II)] to the supporting electrolyte (0.10 mol l^{-1} $NaNO_3$ and 0.10 mol l^{-1} H_3BO_3, pH 4.8). The standard solutions used in the atomic absorption analyses were prepared using a Titrisol standard solution from Merck.

2.2. *Cyclic voltammetry*

Voltammetric experiments under hydrodynamic controlled conditions were carried out in a conventional three-electrode electrochemical cell in order to determine the range of potentials over which the electrochemical reaction is under diffusion control. For this purpose, a model 636 EG&G PAR rotating ring-disc system with a homemade 0.38-cm^2 304-AISI stainless-steel rotating disc electrode (SSRDE) was used. A model 273A EG&G PAR potentiostat/galvanostat controlled by the M270 software was employed for the electrochemical tests. The counter electrode was a large area platinum coil and a saturated calomel electrode (SCE) was used as reference. The SSRDE was polished just before each measurement using 600-grit silicon carbide paper. Cyclic voltammogrames were obtained for this electrode in a 50 ppm Pb(II) solution by cycling the potential between −0.20 and −1.0 V vs. SCE at a scan rate of 10 mV s^{-1} for several rotation rates (600, 1200, 2000, 2800 and 4000 rpm). In order to determine the Pb(II) diffusion coefficient, N_2 was bubbled to eliminate dissolved O_2.

2.3. *Reactor design and procedure for Pb(II) removal*

The system for Pb(II) removal consisted of an electrochemical cell, two 5-l capacity PVC reservoirs for the catholyte and the anolyte, two magnetic recirculation pumps, and two flowmeters to control catholyte and anolyte flow. A scheme of the whole system is shown in Figure 1. The electrochemical cell was mounted using five PVC circular plates in a "sandwich" form. In order

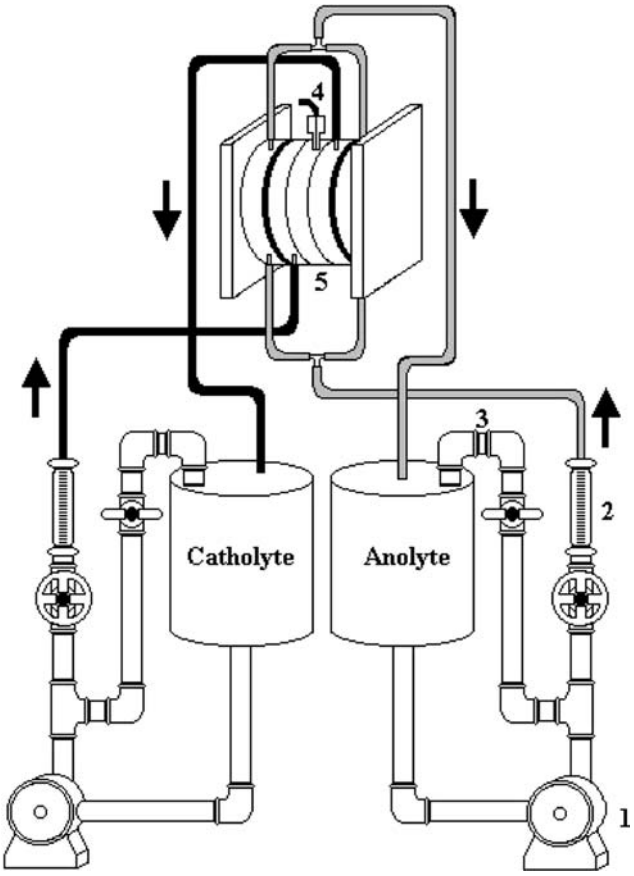

Fig. 1. Schematic representation of the continuous reactor system: (1) pump, (2) flowmeter, (3) bypass, (4) reference electrode (SCE), (5) flow-through cell.

to avoid PbO_2 deposition on the anodes, the cell was divided into one cathodic and two independent anodic compartments separated by two Nafion® 324 membranes (Du Pont), as shown in Figure 2. Between each two Nylon plates of the electrochemical cell, rubber gaskets were placed. The cathodic compartment consisted of two perforated PVC plates (acting as turbulence promoters) and a PVC plate in which an Amway® SSW was attached to a stainless-steel strip placed on the inner side of the plate using a conductive glue made by mixing epoxy resin with graphite powder, 50 wt%. The diameter and thickness of both the cathode compartment and the SSW were the same (7.0 and 1.2 cm, respectively). A copper current feeder was soldered to the stainless-steel strip. Two stainless-steel plates (15.0 × 15.0 × 0.5 cm) were used as anodes and a SCE was placed in the cathodic compartment close to the SSW in order to monitor the SSW cathode potential. The main chemical elements of the SSW were determined by induced coupled plasma optical emission spectrometry (ICP OES) and the following mass composition was found: Cr 16.0%, Ni 0.11%, Mn 0.36% and Si 0.45%. This composition indicates that SSW is possibly a ferrite steel.

All experiments were carried out in the recirculation mode of operation. The catholyte reservoir was loaded

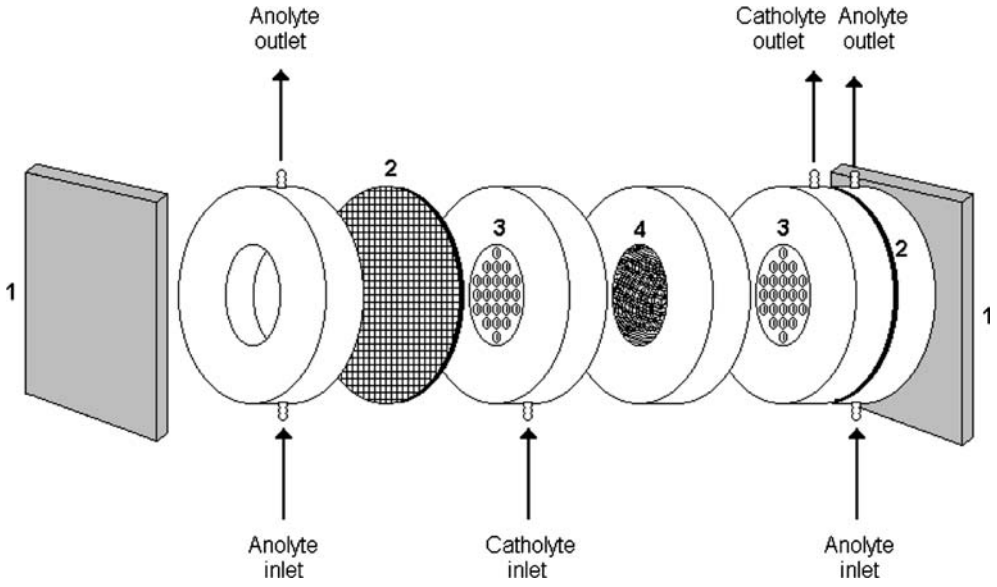

Fig. 2. Expanded view of the cell with a SSW cathode: (1) stainless steel anodes, (2) cationic membranes, (3) turbulence promoters and (4) stainless-steel wool.

with 2 l of the supporting electrolyte solution containing 50 ppm Pb(II) without bubbling N_2 to eliminate dissolved O_2. The anolyte (supporting electrolyte) was placed in a separate reservoir. The system was potentiostatically controlled by an Eco Chemie Autolab/PGSTAT 30 galvanostat/potentiostat connected to a microcomputer with a GPES software. The decrease of the Pb(II) concentration was studied at different flow rates (65, 150 and 250 l h^{-1}) and potentials taken from the limiting-current plateaux obtained in the voltammetric experiments. At predetermined times, the Pb(II) concentration was determined by sampling the catholyte and analyzing it by atomic absorption spectrometry (Varian SpectrAA 200 spectrometer, using an air/acetylene flame).

3. Results and discussion

3.1. *Cyclic voltammetry*

Figure 3 shows a series of cyclic voltammogrames (−0.20 to −1.0 V vs. SCE) obtained for SSRDE at different rotation rates in a solution containing 200 ppm of Pb(II)

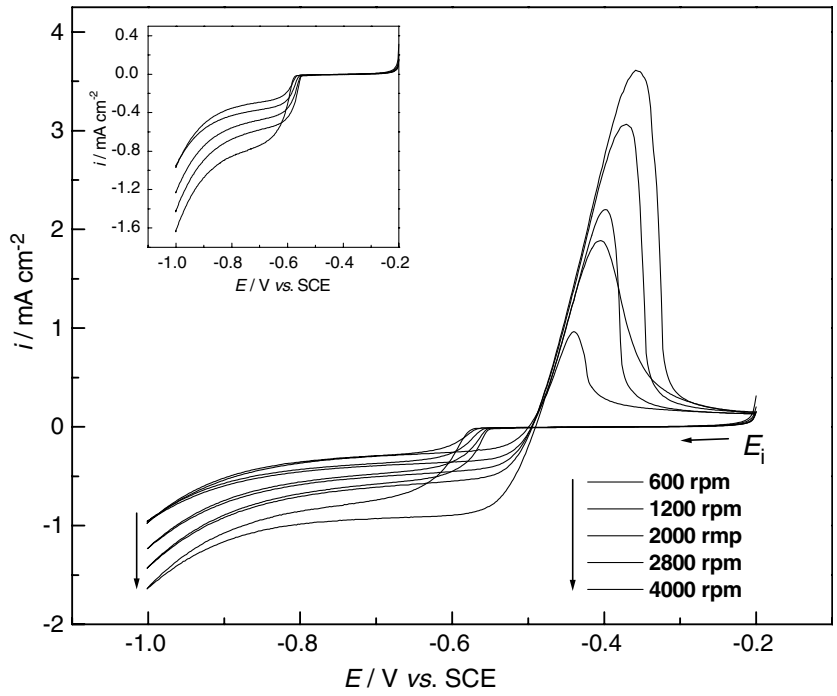

Fig. 3. Cyclic voltammogrames obtained for a 304-AISI SSRDE in a 0.10 mol l^{-1} $NaNO_3$ and 0.10 mol l^{-1} H_3BO_3 deaerated solution containing 50 ppm of Pb(II). Scan rate of 10 mV s^{-1}. Rotation rates indicated on the graph. Inset: Cathodic portions of the cyclic voltammogrames.

in the deaerated supporting electrolyte. Firstly, these curves indicate that the Pb(II) electroreduction begins around −0.57 V and that a very well defined limiting current plateau is developed for potentials ranging from −0.75 to −0.90 V. The magnitude of the current density is clearly dependent on the SSRDE rotation rate. This behaviour indicates that the reaction is diffusion controlled in this potential range. An increase in current density is observed for more negative potentials due to the hydrogen evolution reaction. In the cathodic portion of the reverse scan, the current density values are higher than those recorded in the forward scan, which is characteristic of a process involving nucleation and growth of a lead phase on the stainless-steel electrode [11]. In the reverse scan, the current density becomes positive around −0.50 V and the oxidation peak current is clearly dependent on the SSRDE rotation rate. This behaviour occurs because the flow of Pb(II) species toward the electrode surface was directly dependent on the electrode rotation rate during the forward scan, depositing more lead to be oxidized during the reverse scan.

According to curve (a) in Figure 4, the limiting current density measured at −0.80 V vs. SCE in Figure 3 is proportional to the square root of the rotation rate, obeying a linear relationship. As can be seen from these Levich plots, at this potential (and at more negative ones), the electrodeposition process is mass transfer controlled, a behaviour that is consistent with other literature [13].

During lead electrodeposition the following cathodic reactions should be taken into consideration:

$$Pb^{2+} + 2e^- \rightarrow Pb \qquad E^0 = -0.13\,V \tag{1}$$

$$O_2 + 4H^+ + 4e^- \rightarrow 2H_2O \qquad E^0 = 1.23\,V \tag{2}$$

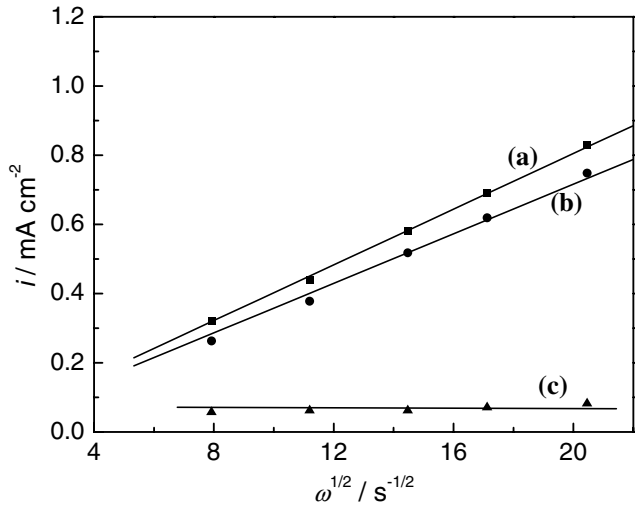

Fig. 4. Levich plots using the limiting current values taken at −0.80 V vs. SCE in the presence (a) and absence (c) of Pb(II). [(b) = (a)–(c)].

$$2H_2O + 2e^- \rightarrow H_2 + 2OH^- \qquad E^0 = -0.83\,V \tag{3}$$

$$NO_3^- + H_2O + 2e^- \rightarrow NO_2^- + 2OH^- \qquad E^0 = 0.01\,V \tag{4}$$

As can be deduced from Equations (2) to (4), the oxygen, water and nitrate reduction reactions are competitive parallel processes. Thus, in order to correctly determine the Pb(II) diffusion coefficient in the supporting electrolyte, it was necessary to bubble N_2 in the solution to eliminate dissolved O_2 and to discount the water and nitrate reaction contributions to the total current density in the cyclic voltammogrames shown in Figure 3. Using the supporting electrolyte without lead, new voltammogrames (not shown) were recorded under the same conditions as those employed to obtain the data shown in Figure 3, so that the current densities recorded under these conditions (−0.80 V vs. SCE) resulted exclusively from the reduction of the water and nitrate (background current density), as shown in Figure 4 (curve c). This curve also shows that the current densities related to these reduction processes are practically independent of the SSRDE rotation rate, which was expected due to their very high concentrations. This value of background current density was discounted from the values of total current density in Figure 3, resulting in current density values for the Pb(II) reduction shown in Figure 4 (curve b). Data from the last curve were used to estimate the Pb(II) diffusion coefficient, using the Levich equation:

$$i_L = 0.62nFD^{2/3}C(0)\omega^{1/2}\nu^{-1/6} \tag{4}$$

where n is the number of electrons involved in the reaction, F the Faraday constant, $C(0)$ the Pb(II) bulk concentration, D the diffusion coefficient, ω the rotation rate and ν the kinematic viscosity. Assuming the value of the electrolyte kinematic viscosity as equal to 1.0×10^{-2} cm^2 s^{-1} [13], the Pb(II) diffusion coefficient was estimated to be 1.4×10^{-5} cm^2 s^{-1}. This value is in a good agreement with the literature since diffusion coefficients of metallic ions in diluted aqueous solutions present small differences, as can be seen in literature [19, 20]. Bertazzoli et al. [13] and Ragnini et al. [7] reported the values of 2.0×10^{-5} cm^2 s^{-1} and 7.0×10^{-5} cm^2 s^{-1}, respectively, for Pb(II) in electrolytes similar to the one used in this work. The diffusion coefficient of Cu(II) in sulphate medium is 4.9×10^{-5} cm^2 s^{-1} [21] and the value of 4.0×10^{-5} cm^2 s^{-1} was reported for Co(II) in the same medium [22].

3.2. *Removal of lead*

Electrowinning experiments were carried out in a batch recirculation mode of operation under potentiostatic conditions at 25 °C. The cell performance was evaluated for three different potentials (−0.70, −0.80 and −0.90 V

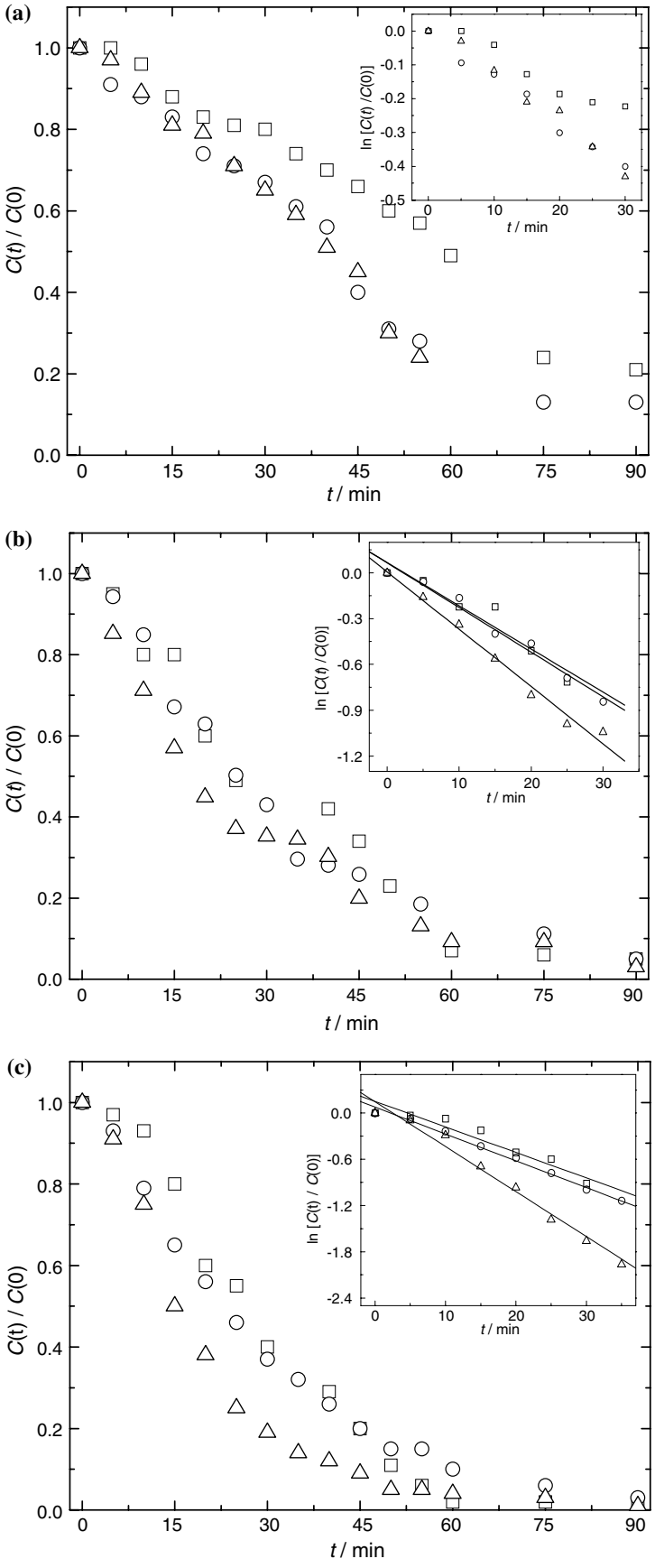

Fig. 5. Normalized concentration $C(t)/C(0)$ vs. time behaviour in the flow-through cell for potentials of (a) −0.70 V, (b) −0.80 V and (c) −0.90 V vs. SCE using the flow rates of 65 l h^{-1} (□), 150 l h^{-1} (○) and 250 l h^{-1} (ρ). Insets: Logarithm of the dimensionless lead concentration against electrolysis time.

vs. SCE) in order to investigate how potential changes affect the cell performance. Nine experiments resulting from the combination of these applied potentials and three electrolyte flow rates (65, 150 and 250 l h^{-1}) were performed. Figure 5 shows the normalized Pb(II) concentration decay as a function of electrolysis time obtained for these different potentials and catholyte flow rates.

As the reaction takes place, an exponential concentration decay is expected for a cell in which the whole electrode surface is operating under mass transport control, as predicted by Equation (5) [23]:

$$C(t) = C(0)\exp\left[-\frac{k_m A_C V_C t}{V_R}\right] \quad (5)$$

where $C(t)$ is the Pb(II) concentration at time t, $C(0)$ the initial Pb(II) concentration, k_m the mass transport coefficient, A_C the specific cathode area (the active area per unit volume of the cathode), V_C the electrode volume and V_R the electrolyte volume.

For the data obtained at −0.70 V (Figure 5a), the Pb(II) concentration decay is not exponential, which suggests that the cathode surface is not completely operating under mass transfer controlled conditions. This is confirmed by the fact that the plots $\ln[C(t)/C(0)]$ vs. time (shown in the inset) are not linear. It is well known from the literature that there is a potential distribution within these porous electrodes that strongly depends on their thickness [8]. Also, studies carried out by Lanza et al. [24] on Zn(II) removal using RVC as cathode showed that the current penetration depends on the electrode thickness, reinforcing the predictions made by Doherty et al. [8]. Therefore, at −0.70 V the reaction may be under mixed control due to potential distribution. Table 1 shows that a small increase in the removal efficiency occurred as the flow rate increased. Only 35% of removal was achieved after a 30-min electrolysis for the highest flow rate.

For more negative potentials (−0.80 and −0.90 V), an exponential decay was observed (see Figures 5b and c), which means that greater cathode surface areas are negatively polarized at these potentials, leading to mass transfer control. This is confirmed by the linearity of the $\ln[C(t)/C(0)]$ vs. time curves (shown in the figure insets), whose slopes are indicatives of the cell performance as they are related to the mass transfer coefficient [23]:

$$s = -k_m A_C V_C / V_R \quad (6)$$

Table 1. Percentage of lead removed from the solution for the different applied potentials and flow rates, for 30-min electrolyses

Potential/V	Flow rate/l h^{-1}		
	65	150	250
−0.70	20	33	35
−0.80	53	57	65
−0.90	60	63	81

Electrolyte: 50 ppm Pb(II) in aerated 0.10 mol l^{-1} $NaNO_3$ and 0.10 mol l^{-1} H_3BO_3, pH 4.8.

Table 2. Values of the slopes (in min^{-1}) of the $\ln[C(t)/C(0)]$ vs. time curves, calculated from the insets in Figure 5b, c.

Potential/V	Flow rate/l h^{-1}		
	65	150	250
−0.80	2.8×10^{-2}	2.9×10^{-2}	3.7×10^{-2}
−0.90	3.3×10^{-2}	3.5×10^{-2}	5.8×10^{-2}

Since A_C, V_C and V_R remain constant throughout the experiment, any slope change is due to variations in the mass transfer coefficient, reflecting the cell performance. The increasing values of the slopes as a function of flow rate are presented in Table 2. As expected, higher removal efficiency values are found (see Table 1). After a 30-min electrolysis at the flow rate of 250 l h^{-1}, 65% removal was achieved at −0.80 V and 81% at −0.90 V. The current efficiencies were less than 20% (see Table 3) due to hydrogen evolution, oxygen and nitrate reduction, which take place simultaneously with the Pb(II) reduction and consume most of the charge. Other authors investigated the removal of different metals using RVC cathodes in aerated solutions and also found low values for the current efficiency [6, 10, 11, 13]. It is important to point out that the reduction of dissolved O_2 must be the predominant process that contributes for the low values of current efficiency. Assuming air-saturated water and mass transport limiting conditions, the O_2 limiting current density can be estimated by Equation (4) using the value of 2.3×10^{-5} cm^2 s^{-1} for O_2 diffusion coefficient [20]. A value of 0.81 mA cm^{-2} is found for 4000 rpm, which is practically the same value observed for Pb(II) reduction without dissolved O_2 in the solution (see curve a of Figure 4). This prediction was experimentally confirmed. For a given rotation rate, the values of the limiting current density in the presence of dissolved O_2 were always almost twice the ones obtained in its absence.

In studies carried out by Elsherief [18] on the removal of Cd(II) using a spiral wound steel electrode, similar concentration decay curves were obtained. When 250 μA cm^{-2} was applied to the electrode, an exponential concentration decay was not observed, but it was for 400 μA cm^{-2}. Other authors have usually found exponential concentration decay under mass transfer conditions [6, 7, 10–13].

Table 3. Current efficiencies for the different applied potentials and flow rates, for a 30-min electrolysis

Potential/V	Flow rate/l h^{-1}		
	65	150	250
−0.70	13 (131.8)	17 (181.0)	16 (171.0)
−0.80	10 (393.7)	17 (329.7)	17 (370.8)
−0.90	16 (344.2)	13 (382.3)	17 (484.8)

The total charges (in coulombs) involved in each electrolysis are indicated in parenthesis. Electrolyte: 50 ppm Pb(II) in aerated 0.10 mol l^{-1} $NaNO_3$ and 0.10 mol l^{-1} H_3BO_3, pH 4.8.

For the electrolysis carried out at −0.90 V and 250 l h^{-1} (Figure 5c), 90% removal was achieved after 45 min; furthermore, after 90 min, a concentration of only 1 ppm was reached, which corresponds to 98% reduction. These conditions were found to be the best for Pb(II) removal with the system used in this work. It should be emphasized that higher removal efficiencies could be achieved for higher flow rates and/or electrolysis times.

4. Conclusions

Voltammetry under hydrodynamic conditions was used to determine the Pb(II) diffusion coefficient, which was estimated to be 1.4×10^{-5} cm^2 s^{-1} in the electrolyte used in this work. Hydrogen evolution and oxygen reduction were shown to be important parasitic reactions that cause a decrease in current efficiency. The Pb(II) reduction process is not completely mass transfer controlled at −0.70 V vs. SCE. On the other hand, the Pb(II) concentration decay was exponential for potentials of −0.80 V and −0.90 V, which implies a mass transfer control. The removal of Pb(II) was proved possible through electrodeposition on a SSW cathode from $NaNO_3$—H_3BO_3 solutions at pH 4.8. The most efficient Pb(II) removal electrolysis was achieved for a flow rate of 250 l h^{-1} at −0.90 V vs. SCE, when the Pb(II) concentration decayed from 50 ppm to only 1 ppm in 90 min, which corresponds to 98% removal.

Acknowledgements

The authors thank CAPES, CNPq and FAPESP for financial support.

References

1. S.E. Daniel, C.P. Pappis and T.G. Voutsinas, *Resour. Conserv. Recycl.* **37** (2003) 251.
2. F.C. Walsh, *Pure Appl. Chem.* **73**(12) (2001) 1819.
3. L.C. Ferracin, A.E.C. Sanhueza, R.A. Davoglio, L.O. Rocha, D.J. Caffeu, A.R. Fontanetti, R.C. Rocha-Filho, S.R. Biaggio and N. Bocchi, *Hydrometallurgy* **65**(2–3) (2002) 137.
4. K. Jüttner, U. Galla and H. Schmieder, *Electrochim. Acta* **45** (2000) 2575.
5. R. Alkire and B. Gracon, *J. Electrochem. Soc.* **122** (1975) 1594.
6. A.J.B. Dutra, A. Espínola and P.P. Borges, *Miner. Eng.* **13**(10–11) (2000) 1139.
7. C.A.R. Ragnini, R.A. Di Iglia, W. Bizzo and R. Bertazzoli, *Water Res.* **34**(13) (2000) 3269.
8. T. Doherty, J.G. Sunderland, E.P.L. Roberts and D.J. Pickett, *Electrochim. Acta* **41**(4) (1998) 519.
9. R.E. Sioda and H. Piotrowsca, *Electrochim. Acta* **25** (1980) 331.
10. J. Tramontina, D.S. Azambuja and C.M.S. Piatnick, *J. Braz. Chem. Soc.* **13**(4) (2002) 469.
11. R.C. Widner, M.F. Souza and R. Bertazzoli, *J. Appl. Electrochem.* **28** (1998) 201.
12. C. Ponce De Leon and D. Pletcher, *Electrochim. Acta* **41**(4) (1996) 533.
13. R. Bertazzoli, C.A. Rodrigues, E.J. Dallan, M. Fukunaga, M.R.V. Lanza, R.R. Leme and R.C. Widner, *Braz. J. Chem. Eng.* **15**(4) (1998) 396.
14. E.C. Weakly and H. Dicamillo, Apparatus and process for recovering metals from aqueous solutions, Patent US 99-248064 (RRT 10 Box 480, Glenwood, NM 88039, 2001).
15. D. Barnes and T.R. Raponi, *Miner. Metall. Process.* **8**(3) (1991) 128.
16. M. Paidar, K. Bouzek, M. Laurich and J. Thonstad, *Water Environ. Res.* **72**(5) (2000) 618.
17. L.A.D. Barbosa, L.G.S. Sobral and A.J.B. Dutra, *Miner. Eng.* **14**(9) (2001) 963.
18. A.E. Elsherief, *Electrochim. Acta* **48** (2003) 2667.
19. R. Greef, R. Peat, L.M. Peter and D. Pletcher, *Instrumental Methods in Electrochemistry* (Ellis Horwood, Chichester, 1990).
20. H.B. Oldham and J.C. Myland, *Fundamentals of Electrochemical Science* (Academic Press, Inc, 1994).
21. D. Pletcher, I. White, F.C. Walsh and J.P. Millington, *J. Appl. Electrochem.* **21** (1991) 659.
22. R. Bertazzoli and M.F.B. Souza, *J. Braz. Chem. Soc.* **8**(4) (1997) 357.
23. A.T.S. Walker and A.A. Wragg, *Electrochim. Acta* **22** (1977) 1129.
24. Lanza and R. Bertazzoli, *J. Appl. Electrochem.* **30**(1) (2000) 61.